The MET oncogene is a functional marker of a glioblastoma stem cell subtype.

UNIVERSITÀ DEGLI STUDI DI TORINO

The *MET* Oncogene Is a Functional Marker of a Glioblastoma Stem Cell Subtype

Francesca De Bacco1, Elena Casanova1, Enzo Medico1, Serena Pellegatta2,4, Francesca Orzan1, Raffaella Albano1, Paolo Luraghi1, Gigliola Reato1, Antonio D'Ambrosio1, Paola Porrati2, Monica Patanè2, Emanuela Maderna3, Bianca Pollo3, Paolo M. Comoglio1, Gaetano Finocchiaro2,4, and Carla Boccaccio1

Authors' Affiliations: [1]IRCC–Institute for Cancer Research, Center for Experimental Clinical Molecular Oncology, University of Turin Medical School, Candiolo; [2]Unit of Molecular Neuro-Oncology, [3]Unit of Neuropathology, Fondazione I.R.C.C.S. Istituto Neurologico C. Besta; and [4]Department of Experimental Oncology, IFOM-IEO Campus, Milan, Italy

Corresponding Authors:
Carla Boccaccio, IRCC, University of Torino Medical School, Str. Prov. 142, Candiolo, 10060, Italy. Phone: 39-011-993-3208; Fax: 39-011-993-3225; E-mail:carla.boccaccio@ircc.it; and Paolo M. Comoglio. Phone: 39-011-9933601; E-mail:antonella.cignetto@ircc.it

Abstract

The existence of treatment-resistant cancer stem cells contributes to the aggressive phenotype of glioblastoma. However, the molecular alterations that drive stem cell proliferation in these tumors remain unknown. In this study, we found that expression of the *MET* oncogene was associated with neurospheres expressing the gene signature of mesenchymal and proneural subtypes of glioblastoma. Met expression was almost absent from neurospheres expressing the signature of the classical subtype and was mutually exclusive with amplification and expression of the EGF receptor (*EGFR*) gene. Met-positive and Met-negative neurospheres displayed distinct growth factor requirements, differentiated along divergent pathways, and generated tumors with distinctive features. The Met^{high} subpopulation within Met-pos neurospheres displayed clonogenic potential and long-term self-renewal ability *in vitro* and enhanced growth kinetics *in vivo*. In Met^{high} cells, the Met ligand HGF further sustained proliferation, clonogenicity, expression of self-renewal markers, migration, and invasion *in vitro*. Together, our findings suggest that Met is a functional marker of glioblastoma stem cells and a candidate target for identification and therapy of a subset of glioblastomas.

Introduction

Glioblastoma, the highest grade glioma variant, is a relatively rare (yearly incidence of 4–5/100,000 people) but very aggressive tumor, associated with high morbidity, mortality, and recurrence (median survival of 12–15 months; ref. 1). These meager treatment options prompted a huge effort to achieve comprehensive profiling of gene expression patterns and genetic alterations (2–6), in order to identify molecular targets for innovative—possibly personalized—therapies. By expression profiling, 3 main glioblastoma subtypes have been recognized: classical, mesenchymal, and neural/proneural (here proneural; ref. 6). The classical subtype mostly displays alterations of the EGF receptor (*EGFR*) gene, such as amplification or deletion of the extracellular domain ($EGFR^{vIII}$; ref. 6). The mesenchymal subtype often harbors a normal *EGFR* gene and deletion of *NF1* or *PTEN*tumor suppressor genes (6). The proneural subtype preferentially associates with mutations of isocitrate dehydrogenase 1 (*IDH1*) or 2 (*IDH2*), or aberrant activation of PDGFRA, resulting from gene amplification/mutation, or occurrence of autocrine loops. This subtype, often evolving from lower grade gliomas, may associate with a more favorable prognosis, but does not benefit from current therapies (6, 7).

To understand glioblastoma pathogenesis, it is crucial to identify the driving genetic lesions and to recognize that glioblastoma onset and progression depend on a (small) subpopulation of cancer stem cells (CSC), which, according to an operational definition, hold replicative immortality *in*

vitro and tumor-initiating potential when transplanted *in vivo*(8, 9). Despite the controversy arising on the ultimate, elusive nature of these cells, convincing evidence indicates that CSCs possess inherent radio- and chemoresistance, a major cause of treatment failure and disease recurrence (10, 11). To envisage new therapeutical strategies, genetic and molecular alterations occurring in glioblastoma stem cells must be identified. Therefore, we investigated whether the molecular alterations detectable in the clinically manifest glioblastoma were present in the tumor-initiating subset, allowing classification in subtypes already at the CSC level. From primary glioblastoma tissues, we isolated and propagated extensively self-renewing neurospheres, that is, cultures enriched in stem and progenitor cells (12). These neurospheres displayed mutational profiles largely overlapping with those of the original tumors and could be classified as classical, mesenchymal, or proneural, according to their gene expression profile. We then specifically associated expression of the *MET* oncogene with mesenchymal and proneural neurospheres, and we showed that Met signaling actively supported the stem-like and invasive phenotype.

Materials and Methods

Neurospheres derivation and culture

Neurospheres were derived from glioblastoma specimens diagnosed according to WHO criteria (13) and cultured in standard medium containing EGF and bFGF (12). HGF (20 ng/mL) was added where indicated.

Evaluation of tumorigenicity

Cells were injected ortothopically (2×10^5 cells) or subcutaneously (10^5 cells in v/v PBS/Matrigel) into 6 weeks old male NOD.CB17-$Prkdc_{scid}$/J mice.

Gene copy number and sequencing

Gene amplification was assessed using commercially available TaqMan Copy Number Assays. For gene sequencing, specific primer pairs used are listed in Supplementary Table S7.

Microarray data

Data have been deposited in the GEO database, accession number GSE36426.

Immunophenotypical analysis and fluorescence-activated cell sorting

Cells were incubated with the antibodies listed in Supplementary Table S8.

Proliferation assay

Cells were plated at clonal density (10 cells/μL) in 96-well plates in a medium devoid of growth factors. Twenty-four hours after seeding (day 0), the indicated growth factors were added, and proliferation was measured by Cell Titer Glo.

Clonogenic assay and long-term propagation

Single cells were directly sorted into 96-well plates (1 cell/well). Neurospheres were counted 14 days after seeding. For long-term propagation, cells were plated at clonal density, and formed neurospheres were dissociated, counted, and replated once a week.

Migration and invasion assays

A total of 10^5 cells were seeded in Transwell in the absence (migration) or in the presence (invasion) of Matrigel (10 μg/cm^2; ref. 14).

Statistical analysis

Numerical results were expressed as means ± SEM. Statistical significance was evaluated using 2-tailed Student *t* tests, Fisher exact tests or $Ç^2$ tests. Multiple comparisons were carried out using Bonferroni correction. Values of *P* less than 0.05 were considered statistically significant.

For the other methods see Supplementary Experimental Procedure.

Results

Neurospheres harbor genetic lesions specific of glioblastoma subtypes

Eighteen neurospheres were randomly chosen from an ample panel of neurospheres derived from surgical specimens of primary glioblastomas (WHO grade IV; ref. 13; Table 1). Histologic sections of the corresponding tumors were analyzed for mitotic index (invariably high, data not shown), EGFR, and p53 expression (15), and traits associated with subtyping, including vascular stroma proliferation and YKL-40 expression (ref. 5;Table 1 and Supplementary Fig. S1A).

Table 1.

Clinical and neuropathologic data of primary glioblastoma (WHO grade IV)

Patient code	Gender	Age	OS (wks)	Location	EGFR	Nuclear p53	Vascular stroma proliferation	YKL-40
BT358	F	63	89	F dx	0	0	1+	2+
BT273	M	58	55	FTP dx	2+	2+	0	0
BT275	F	66	60	P dx	0	0	1+	0
BT373	M	63	60	F dx	0	1+	0	0
BT334	M	63	42	FT dx	1+	0	0	0
BT297	M	54	61	T sx	1+	0	0	3+
BT168	F	78	39	PO sx	1+	0	1+	1+
BT326	M	27	27	F sx	0	0	2+	2+
BT332	M	74	41	PO sx	1+	0	1+	1+
BT347	F	57	12	T sx	1+	1+	2+	0
BT337	M	63	76	FTP sx	0	0	0	0
BT328	M	54	78	F sx	n.a.	n.a.	n.a.	n.a.
BT299	M	49	31	TPO sx	0	0	1+	2+
BT379	M	73	12	FTP dx	0	0	1+	0
BT205	M	73	8	T dx	0	0	1+	2+
BT302	F	18	127[a]	FP dx	0	1+	2+	2+
BT308	M	76	22	T sx	0	1+	1+	1+
BT314	M	67	76	T sx	0	1+	1+	1+

NOTE: Immunohistochemistry scores, 3+, intensive positive; 2+, positive; 1+, focally positive; 0, no staining.

Abbreviations: OS, overall survival (wks); n.a., not assessed.

- [a]Alive January 2012.

Table 1.
Clinical and neuropathologic data of primary glioblastoma (WHO grade IV)

Neurospheres and their corresponding tumors were analyzed for the presence of genetic alterations known occurring at high frequency in glioblastoma, such as amplification of*EGFR* ($EGFR^{amp}$), or deletion of its extracellular domain (exon 2–7, $EGFR^{vIII}$), amplification of *PDGFRA*, mutations of *IDH1/2*, *TP53,* *PTEN*, and *NF1* (refs. 6, 16; Table 2; *EGFR* and *PDGFRA* gene copy number and expression of $EGFR^{vIII}$ in Supplementary Fig. S1B and C; *TP53*, *PTEN*, and *NF1* mutations in Supplementary Table S1).
View this table:

Table 2.

Genetic lesions in neurospheres (NS) and the corresponding original glioblastoma tissue specimens (T)

Patient code	$EGFR^{amp}$[a]		$EGFR^{vIII}$[a]		$PDGFRA^{amp}$		$IDH1/2^{mut}$		$TP53^{mut}$[b]		$PTEN^{mut}$[b]		$NF1^{mut}$[b]	
	NS	T	NS	T	NS	T	NS	T	NS	T	NS	T	NS	T
BT358	+	+	+	+	–	–	–	–	–	–	–	–	–	n.a.
BT273	+	+	+	+	–	–	–	–	+	+	–	–	–	n.a.
BT275	+	+	–	+	–	–	–	–	+	+	–	–	–	n.a.
BT373	+	+	–	+	–	–	–	–	–	–	–	–	–	n.a.
BT334	+	+	+	+	–	–	–	–	–	n.a.	–	n.a.	–	n.a.
BT297	+	+	–	–	–	–	–	–	–	–	–	–	–	n.a.
BT168	+	+	–	+	–	–	–	–	+	n.a.	–	n.a.	–	n.a.
BT326	+	+	–	–	–	–	–	–	–	–	+	+	–	n.a.
*BT332	–[c]	+	–	+	–	–	–	–	–	–	+	+	–	n.a.
*BT347	–[c]	+	–	–	–	–	–	–	+	+	+	+	–	n.a.
*BT337	–	+	–	–	–	–	–	–	–	–	–	–	–	n.a.
*BT328	–	+	–	–	–	–	–	–	+	+	+	–	–	n.a.
BT299	–[c]	–[c]	–	–	–	–	–	–	–	–	+	+	–	n.a.
*BT379	–	–	–	+	–	–	–	–	+	+	+[d]	+[d]	+	n.a.
BT205	–[c]	–	–	–	–	–	–	–	+	–	+	–	+	n.a.
BT302	–	–[c]	–	–	–	–	–	–	–	–	+	+	–	n.a.
BT308	–[c]	–	–	–	–	–	–	–	+	+	+	+	–	n.a.
BT314	–	–	–	–	–	–	–	–	+	+	+	+	–	n.a.

NOTE: +, presence of genetic alterations; −, absence of genetic alterations.

Abbreviation: n.a., not accessed due to lack of material.

- [a]Analysis of $EGFR^{amp/vIII}$ is shown in Supplementary Fig. S1 and reported in Supplementary Table S2.
- [b]Detailed list of mutations is reported in Supplementary Table S1
- [c]chr7 polysomy
- [d]Homozygous deletion

Table 2.
Genetic lesions in neurospheres (NS) and the corresponding original glioblastoma tissue specimens (T)

Eight of 18 neurospheres displayed *EGFR* amplification and/or deletion ($EGFR^{amp/vIII}$), a genetic trait preferentially associated with the “classical” glioblastoma subtype, whereas the remaining harbored a normal *EGFR* gene ($EGFR^{wt}$), usually found in either “mesenchymal” or “proneural” subtypes (ref. 6; Table 2). No neurosphere displayed the genetic landmarks of the “proneural” subtype, such as *PDGFRA* amplification or autocrine loop, or *IDH1/2* mutations (ref. 6; Table 2 and

data not shown). *TP53, PTEN*, or *NF1*alterations (mutations or deletions) were found in 9 of 18, 10 of 18, and 2 of 18 neurospheres, respectively (Table 2 and Supplementary Table S1). Mutations of *TP53* and*NF1* were shown to preferentially associate with $EGFR^{wt}$ glioblastomas (6). In our panel, however, only *PTEN* deletion/mutation was significantly associated with $EGFR^{wt}$ (for*TP53*, Fisher exact test, $P = 0.637$; for *PTEN*, $P = 0.003$; for *NF1*, $P = 0.477$).
Neurospheres displayed a mutational profile largely overlapping with the corresponding original tumors (Table 2). However, 5 of 13 neurospheres derived from $EGFR^{amp/vIII}$ tumors lacked *EGFR* alterations (Table 2). Moreover, in the remaining $EGFR^{amp/vIII}$ neurospheres, the number of *EGFR* gene copies was decreased with respect to the corresponding original tumor (Supplementary Table S2). These findings are consistent with previous reports, indicating that *in vitro* culture selects against *EGFR* genetic lesions (refs. 17, 18; see Discussion).

Neurospheres can be classified as classical, mesenchymal, or proneural according to gene expression profile

Next we carried out genome-wide gene expression profiling of the whole neurosphere panel and assessed whether they could be subdivided in classical, mesenchymal, or proneural subgroups by the transcriptional signature identified in an independent set of glioblastoma tissues by Verhaak (ref. 6; Fig. 1A and Supplementary Fig. S2). The classical, mesenchymal, and proneural centroids (i.e., 3 virtual samples displaying average expression of each signature gene in, respectively, classical, mesenchymal, and proneural glioblastomas) were extracted from the published datasets (https://tcga-data.nci.nih.gov/docs/publications/gbm_exp/) and mapped in the microarray, resulting in 549 probes, corresponding to 532 genes. The 3 centroids and the neurosphere samples were then hierarchically clustered by unsupervised analysis. The clustering sharply subdivided the neurospheres in 3 subgroups, including the classical, the mesenchymal, and the proneural centroid, respectively (Fig. 1A and Supplementary Fig. S2).

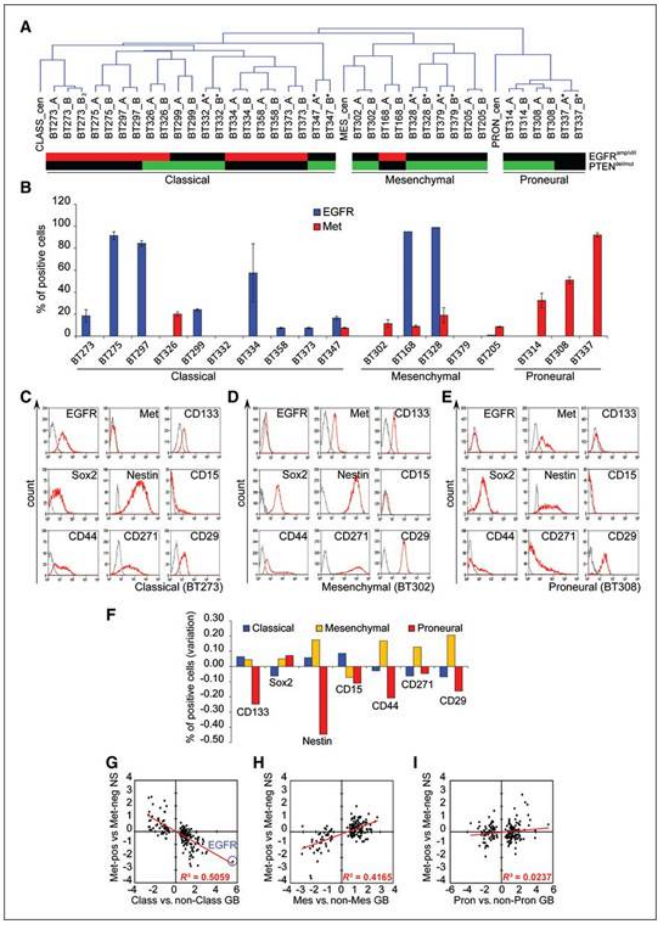

Figure 1.

Neurospheres are classified according to gene expression profile and display subtype-specific EGFR or Met expression. Unsupervised hierarchical clustering of duplicate neurosphere samples (A and B) and classical (CLASS_cen), mesenchymal (MES_cen), or proneural (PRON_cen) centroids. Red cells, amplification/mutation of *EGFR* (*EGFR*$^{amp/vIII}$); green cells, deletion/mutation of *PTEN*(PTEN$^{del/mut}$); black cells, no lesion. *, derived from tumors with EGFR$^{amp/vIII}$; BT273_B_2, technical replicate. B, flow cytometric detection of EGFR or Met in neurospheres. C–E, immunophenotype of neurospheres representative of each subtype. F, variation of the average number of cells positive for the indicated markers in each subtype with respect to all neurospheres (absolute numbers in Supplementary Table S3). G–I, relative expression of 532 signature genes (https://tcga-data.nci.nih.gov/docs/publications/gbm_exp/; black dots). x-axis, log_2 ratio between glioblastoma (GB) samples of each subtype versus the other subtypes; y-axis, log_2 ratio between Met-pos-NS and Met-neg-NS.

By comparing neurosphere gene expression and mutational profiles, we observed that the majority (7 of 10) of neurospheres profiled as classical harbored *EGFR* gene amplification/deletion (EGFR$^{amp/vIII}$; Fig. 1A). Interestingly, the 3 of 10 classical neurospheres without *EGFR* gene amplification displayed high chromosome 7 polisomy and, in 2 cases, derived from EGFR$^{amp/vIII}$ tumors (Table 2). On the contrary, 7 of 8 neurospheres profiled as mesenchymal or proneural harbored a normal *EGFR* gene (EGFR^{wt}; Fig. 1A). Altogether, these data indicated a marked preferential association of EGFR$^{amp/vIII}$ with classical compared with mesenchymal/proneural neurospheres ($Ç^2$ test,$P <$ 0.04). *Vice versa*, although not statistically significant, *PTEN* mutation/deletion was preferentially associated with mesenchymal/proneural compared with classical neurospheres (6 of 8 vs. 4 of 10 neurospheres, $Ç^2$ test, P = 0.31; Fig. 1A).

Classical and mesenchymal/proneural neurospheres are discriminated by EGFR or Met expression

Gene expression profiling and qPCR validation (Supplementary Fig. 3A–C) indicated that not only *EGFR* alteration but also transcription was preferentially associated with classical neurospheres (2-sided *t* test, $P < 0.0001$). *Vice versa*, transcription of the *MET*gene, known to be expressed in a fraction (≅30%) of unclassified human gliomas (19, 20), was preferentially associated with mesenchymal/proneural neurospheres (2-sided *t*test, $P < 0.01$).

To further investigate the role of EGFR and Met as markers of classical and mesenchymal/proneural neurosphere subgroups respectively, we assessed by flow cytometry the cell-surface expression of the 2 receptors in the whole neurosphere panel.

As expected, EGFR was detected in the majority (8 of 10) of classical neurospheres, but only in 2 of 8 mesenchymal/proneural neurospheres (Fig. 1B and Supplementary Table S3). *Vice versa*, Met was expressed by the majority (7 of 8) of mesenchymal/proneural neurospheres, with variable percentages of positive cells (5%–94%), but only in 2 of 10 classical neurospheres (Fig. 1B and Supplementary Table S3). Therefore, EGFR protein expression was strongly preferentially associated with the classical neurosphere subgroup ($Ç^2$ test, $P < 0.001$), whereas Met protein was associated with the mesenchymal/proneural neurosphere subgroup ($Ç^2$ test, $P < 0.02$). Interestingly, Met expression (in the absence of any gene alteration) was detected in the majority of original tumors that generated neurospheres expressing Met, but was mostly absent from tumors that generated neurospheres not expressing Met, and that harbored *EGFR* amplification (Supplementary Table S4).

We then analyzed whether other cell-surface markers could be specifically associated with each neurosphere subgroup. CD133, previously used (21), and more recently questioned (22, 23), as glioblastoma stem cell marker, was inconstantly expressed (0%–90% of positive cells), without association with any subgroup (Fig. 1C–F and Supplementary Table S3). Also expression of Sox2, Nestin, and CD15/SSEA1, 3 markers associated with the neural stem cell phenotype (24), did not display any statistically significant difference among the subgroups (Fig. 1C–F and Supplementary Table S3; for Sox2, $Ç^2$ test, $P = 0.08$; for Nestin, $P = 0.09$; for CD15, $P = 0.314$). Consistently, transcription of *CD133* and *Sox2* and other stem cell markers was comparable in all subgroups (Supplementary Fig. S3D). Finally, cell-surface expression of CD44 (a gene of the mesenchymal signature; refs. 5, 6), or CD271 and CD29 (2 markers of mesenchymal differentiation of neural progenitors; ref. 25), was not preferentially associated with any subgroup (for CD44, $Ç^2$ test, $P = 0.304$; for CD271, $P = 0.982$; for CD29, $P = 0.766$; Fig. 1C–F and Supplementary Table S3).

Taken together, these data indicated that, in neurospheres, expression of EGFR and Met are almost mutually exclusive. By combined flow cytometric analysis, unlike other markers, the 2 receptors are sufficient to separate neurospheres in 2 subgroups: EGFR-pos/Met-neg-NS (hereafter indicated as Met-neg-NS), roughly corresponding to classical neurospheres, and EGFR-neg/Met-pos-NS (hereafter indicated as Met-pos-NS), roughly corresponding to mesenchymal/proneural neurospheres. Consistently, Met-pos-NS, unlike Met-neg-NS, were highly enriched in mesenchymal or proneural, but lacked classical signature genes (Fig. 1G–I). Strikingly, among all these signature genes, *EGFR*was, concomitantly, the most expressed in the classical subtype and the least expressed in Met-pos-NS (Fig. 1G).

Met-pos and Met-neg neurosphere subgroups are identified by multiple transcriptional signatures

Neurosphere gene expression profiles were also analyzed by applying additional transcriptional signatures, including 2 identified in glioblastoma neurospheres (26, 27), 2 in original tumors (5, 28), and 1 in mixed tissues, neurospheres, and cell lines (ref. 29; Supplementary Fig. S4 and Supplementary Table S5). The 5 signatures were almost fully mapped in the microarrays and hierarchically clusterized neurospheres. In all cases, Met-pos-NS and Met-neg-NS were sharply separated into distinct and homogeneous clusters. By applying the 2-cluster signatures, the majority of Met-pos-NS fell into Cluster II (26), or Type II (27), or GSr/lines group (29), whereas the majority of Met-neg-NS fell into Cluster I (26), or Type I (27), or GSf/tumor group (29). By applying

the multicluster signatures generated from tumor tissues (5, 28), Met-pos-NS fell into the most aggressive subgroups (Supplementary Fig. S4 and Supplementary Table S5).

Met-pos and Met-neg neurospheres display subtype-specific growth factor requirements and differentiation patterns

We observed that Met-pos-NS and Met-neg-NS displayed distinctive microscopic features: Met-neg-NS mostly displayed a compact, smooth surface, whereas Met-pos-NS appeared as aggregates of cells with loose intercellular adhesion (Fig. 2A). Moreover, in standard medium, Met-pos-NS displayed a proliferative rate significantly higher than Met-neg-NS (Fig. 2B). We then systematically analyzed the proliferative response to EGF or bFGF, alone or in combination (Fig. 2C–E and Supplementary Fig. S5A). Met-neg-NS were mostly quiescent in the absence of growth factors (data not shown), and, with one exception, were markedly stimulated by EGF, but weakly by bFGF alone; the 2 growth factors were not significantly additive (Fig. 2C and E; median fold increase with EGF = 4.54, with bFGF = 1.45, Supplementary Fig. S5A). *Vice versa*, Met-pos-NS grew in the absence of exogenous growth factors (data not shown), and, with some exceptions, were further stimulated by bFGF, but not by EGF; again, the 2 factors were not additive (Fig. 2D and E; median fold increase with EGF = 0.94, with bFGF = 2.73, Supplementary Fig. S5A).

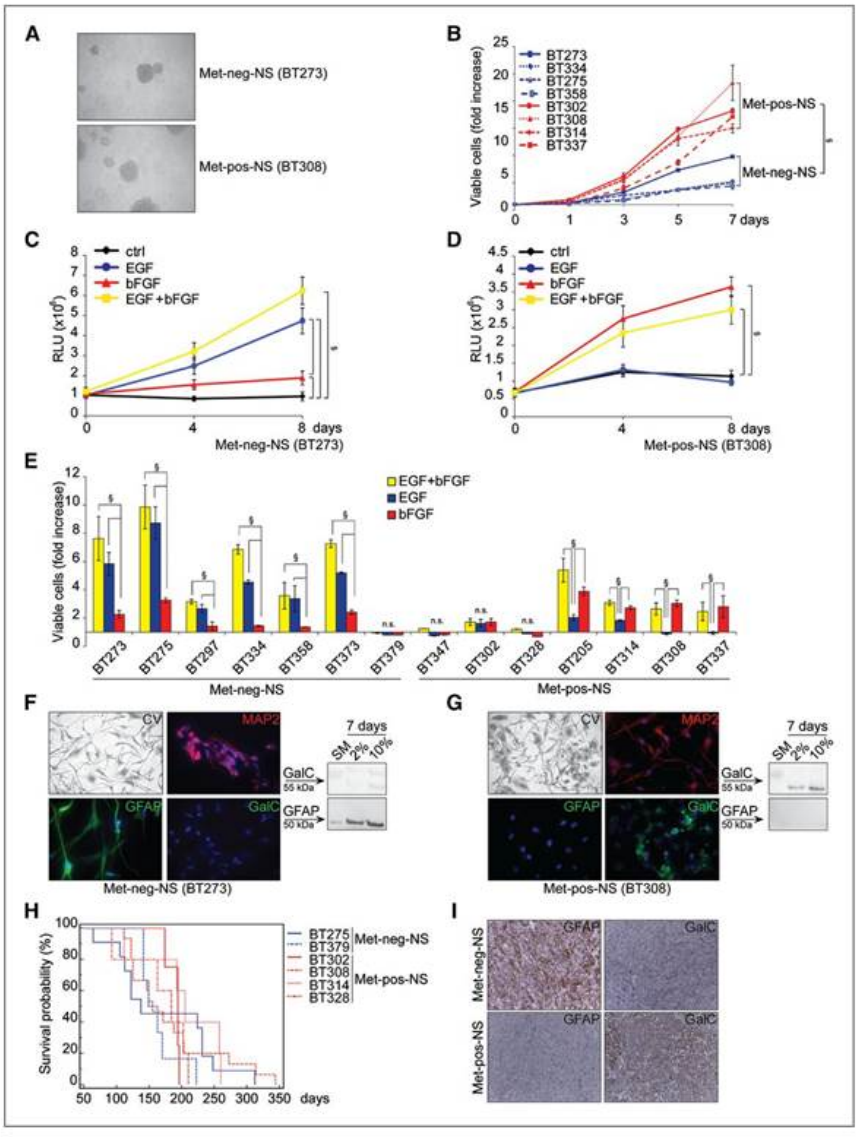

Figure 2.

Met-neg-NS and Met-pos-NS display subtype-specific growth factor requirements and differentiation patterns. A, representative micrographs (magnification, ×100). B, proliferation in standard medium measured by Cell Titer Glo. Fold increase with respect to day 0. §, 2-sided *t* test, $P < 0.05$. C and D, proliferation with different growth factors (EGF and/or bFGF) measured as above. RLU, relative light units. §, 2-sided *t* test, $P < 0.05$. E, proliferation measured as above after 8 days in standard medium (EGF + bFGF) or EGF or bFGF alone, with respect to control cells kept in the absence of growth factors. §, 2-sided *t*test, $P < 0.05$. F and G, micrographs (magnification, ×100) of cells kept in 10% serum for 7 days and stained with crystal violet (CV), or anti-MAP2, anti-GFAP or anti-GalC antibodies. Nuclei counterstained with 4,6-diamidino-2-phenylindole (DAPI). Western blots of cells kept in standard medium (SM) or 2% or 10% serum. H, Kaplan–Meier survival curves of mice orthotopically injected with neurospheres. I, immunohistochemistry for GFAP or GalC in tumors formed by orthotopically injected neurospheres (Met-neg-NS: BT379; Met-pos-NS: BT308, magnification, ×200).

The ability of Met-pos-NS to proliferate in the absence of exogenous growth factors could be explained by expression of autocrine loops (data not shown). The different sensitivity of Met-neg-NS and Met-pos-NS to EGF was correlated with the different levels of EGFR expression (Fig. 1B). Consistently, EGFR family members were found significantly phosphorylated, in the presence of EGF, only in Met-neg-NS (Supplementary Fig. S5C). The comparable sensitivity of both Met-neg and Met-pos neurospheres to bFGF correlated with similar expression and ligand-induced tyrosine phosphorylation of FGFR2, the main bFGF receptor (Supplementary Fig. S5B and C).

By culturing dissociated neurospheres in prodifferentiating conditions, Met-neg and Met-pos neurospheres displayed divergent differentiation patterns (Fig. 2F and G, Supplementary Fig. S5D, and data not shown). Met-neg-NS differentiated into neuro-astroglial lineages, as shown by upregulation of the neural marker MAP2 and the astroglial marker GFAP. No oligodendroglial cells were detected after staining with the specific GalC marker. On the contrary, Met-pos-NS differentiated into neuro-oligodendroglial but not into the astroglial lineage.

Finally, a panel of representative Met-neg and Met-pos neurospheres were orthotopically transplanted into immunocompromised mice. Between the 2 subgroups, no significant differences were reported in mouse survival (Fig. 2H and Supplementary Table S6), tumor proliferative index (Supplementary Table S6), or vascularization (data not shown). In no case, invasion of the contralateral brain hemisphere could be observed (data not shown). However, consistent with the differentiation pattern observed *in vitro*, tumors derived from Met-neg-NS invariably expressed high levels of GFAP, but not GalC. *Vice versa*, those derived from Met-pos-NS invariably expressed high levels of GalC and traces of GFAP only at the tumor periphery (Fig. 2I, Supplementary Table S6, and data not shown).

The above data showed that, although selected and propagated in the same medium, Met-pos and Met-neg neurospheres have distinct, subtype-specific signaling requirements for proliferation and specific differentiation patterns, both *in vitro* and *in vivo*. Altogether, these observations suggested that the corresponding tumors may have different cells of origin (see Discussion).

In Met-pos-NS the Met^{high} subpopulation is enriched with clonogenic and tumorigenic cells

Having established that Met is a marker of a biologically distinct neurosphere subtype, we investigated its functional role. By flow cytometry (Fig. 1B–E and Supplementary Table S3) and immunofluorescence (Fig. 3A and data not shown), we observed that Met expression was restricted to cell subpopulations of various extents, which, in some cases, expressed also high levels of stem cell markers such as Sox2, Nestin, or CD133 (Fig. 3B and data not shown). We thus sorted the Met^{high} from the Met^{neg} subpopulation (for sorting parameters see Supplementary Fig. S6) and carried out clonogenic assays by plating and culturing single cells in standard medium. In 9 of 9 Met-pos-NS, Met^{high} cells invariably displayed higher clonogenic ability as compared with Met^{neg} cells (Fig. 3C and data not shown). Moreover, neurospheres derived from Met^{high} cells maintained their clonogenic ability and differentiative multipotentiality through more than 20 serial passages, whereas those derived from Met^{neg} cells arrested their growth within 3 to 8 passages

(Supplementary Fig. S7A and B). Cell-cycle analysis of the representative neurospheres BT308 showed that, immediately after sorting, the Met^{high} subpopulation contained a higher percentage of cells in the S phase (8.2% vs. 3.4%) and a lower percentage of apoptotic cells (3.4% vs. 20.7%), as compared with the Met^{neg}subpopulation (overlapping results were obtained with BT337, data not shown). In another set of experiments, Met^{high} and Met^{neg} cells were sorted, plated at clonal density, and cultured in standard medium. The secondary clones were analyzed by flow cytometry for Met expression after 7 and 14 days; the clones formed by Met^{high} cells progressively reacquired the same Met immunophenotypic profile (including Met^{high} and Met^{neg}) as the parental neurospheres (Fig. 3D, Supplementary Fig. S7C, and data not shown). In contrast, neurospheres formed by Met^{neg} cells remained entirely composed of Met^{neg}cells.

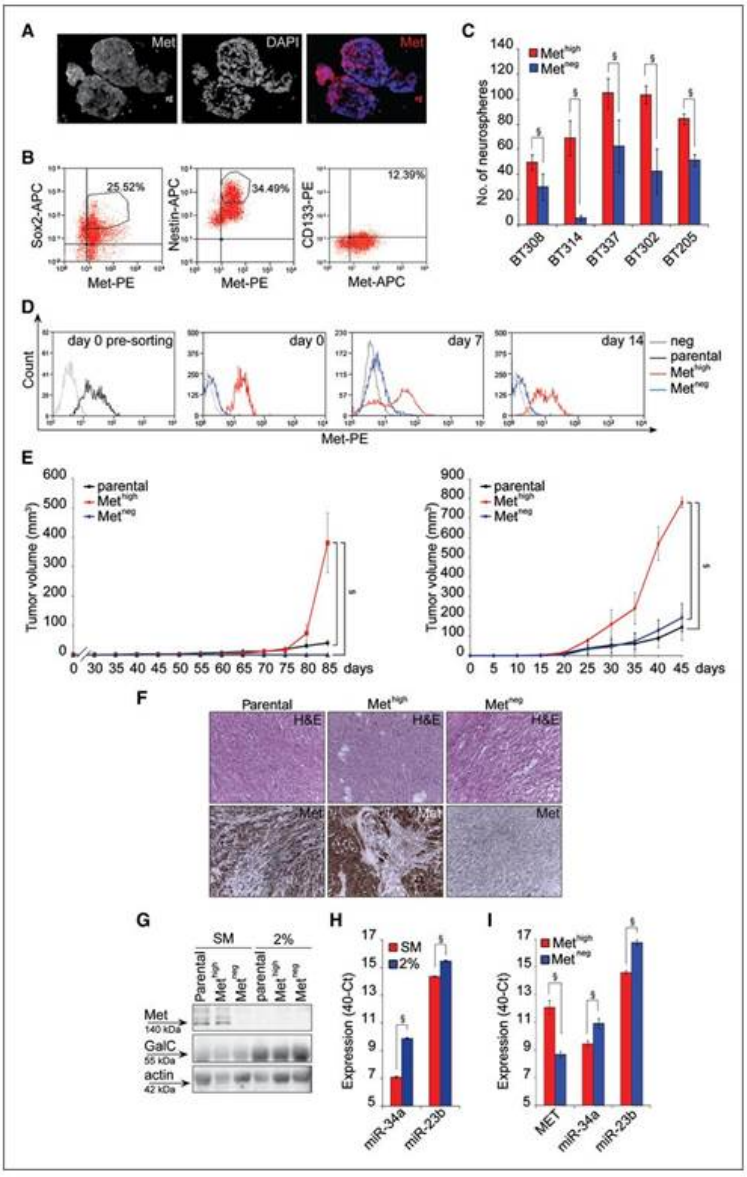

Figure 3.
The Met^{high} subpopulation is enriched with clonogenic and tumorigenic cells. A, Met staining in a representative Met-pos-NS (BT308; magnification, ×400). B, flow cytometry; coexpression of Met with Sox2, Nestin, or CD133 in a representative Met-pos-NS (BT308). C, clonogenic assay; number of neurospheres formed by Met^{high} or Met^{neg} cells after 14 days in standard medium. §, 2-sided *t* test, $P < 0.05$. D, flow cytometry; Met expression analyzed in the unsorted (parental) BT308 neurosphere (black line) at day 0 presorting and in its sorted Met^{high} (red line) and Met^{neg} (blue line) subpopulations at the indicated days after sorting. E, volume of subcutaneous tumors formed by BT308 (left) and 302

(right) neurospheres (parental) and their sorted subpopulations (n = 3 in each group). §, 2-sided t test, $P < 0.05$. F, hematoxylin and eosin (H&E) and Met immunohistochemical staining (magnification, ×200) of the above tumors. Enlarged images in Supplementary Fig. S8. G, Met and GalC expression in BT308 neurosphere (parental) and its sorted subpopulations, 7 days after culture in standard medium (SM), or in prodifferentiating medium (2% serum). H, qPCR of miR-34a and miR-23b transcripts in BT308 neurosphere grown as in G. §, 2-sided t test, $P < 0.05$. I, qPCR of MET, miR-34a, and miR-23b transcripts in the Met^{high} and Met^{neg} subpopulations immediately after sorting from BT308 neurosphere. §, 2-sided t test, $P < 0.05$.

To investigate the tumorigenicity of the 2 subpopulations, representative parental Met-pos-NS (BT308 and BT302) and their sorted Met^{high} or Met^{neg} subpopulations were subcutaneously injected into immunocompromised mice. In the case of BT308, only the parental neurosphere and the Met^{high} subpopulation displayed the ability to form tumors, whereas in the case of BT302, even the Met^{neg} subpopulation generated measurable tumors. However, in both cases, tumors formed by Met^{high} cells grew significantly more rapidly than those formed by the parental or its sorted Met^{neg} subpopulation (Fig. 3E). Interestingly, tumors derived by Met^{high} or unsorted cells had a similar histopathologic aspect, featuring a mixture of small-rounded and spindle-shaped cells. By immunohistochemistry, the small-rounded cells were positive for Met expression, whereas spindle-shaped cells were negative. On the contrary, tumors derived by Met^{neg} cells sorted from BT302 only contained uniform spindle-shaped cells negative for Met expression (Fig. 3F, Supplementary Fig. S8, and data not shown).

Taken together, these findings indicated that, unlike the Met^{neg} subpopulation, the Met^{high} retained long-term clonogenic properties *in vitro*, enhanced growth kinetics *in vivo*, and generated a heterogeneous progeny, including Met^{high} and Met^{neg} cells, both *in vitro* and *in vivo*. Whereas Met^{high} might correspond to stem-like cells, Met^{neg} likely correspond to more differentiated cells that exhaust their proliferative potential. Consistently, we observed that Met expression was downregulated when neurospheres (or the sorted Met^{high} subpopulations) were cultured in prodifferentiating conditions (Fig. 3G and Supplementary Fig. S7D). Concomitantly, upregulation of miRNA-34a and miRNA-23b, both targeting the *MET* transcript (30, 31), was observed (Fig. 3H and data not shown). Interestingly, in neurospheres cultured in standard medium, the same miRNAs were more expressed in Met^{neg} than Met^{high} cells (Fig 3I and Supplementary Fig. S7E).

HGF sustains clonogenicity, expression of self-renewal markers, and cell invasionin vitro

Next we investigated whether HGF stimulated proliferation of Met-pos-NS and their sorted Met^{high} and Met^{neg} subpopulations. When supplied to parental neurospheres as the sole growth factor, HGF displayed a negligible proliferative effect, if compared with bFGF (Fig. 4A and Supplementary Fig. S9A). However, in the sorted Met^{high} subpopulation, HGF significantly increased proliferation, although less intensely than bFGF (2-fold versus 6-fold increase; Fig. 4A and Supplementary Fig. S9A). As expected, HGF did not stimulate proliferation of Met^{neg} cells (Fig. 4A and Supplementary Fig. S9A) and Met-neg-NS (data not shown).

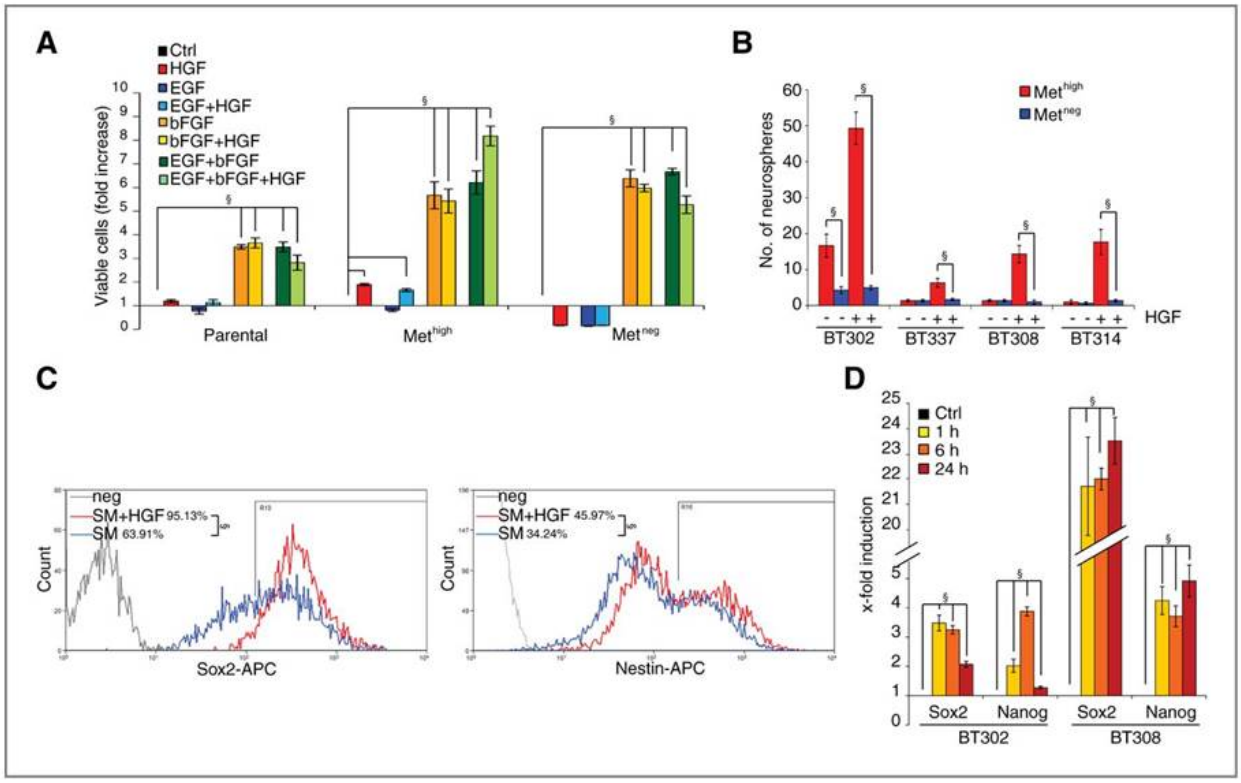

Figure 4.

HGF sustains clonogenicity and expression of self-renewal markers. A, proliferative effect of growth factors on the Met-pos-NS BT308 (parental) or its sorted subpopulations, with respect to control (no growth factor), after 8 days of culture. §, 2-sided *t* test,$P < 0.05$. B, clonogenic assay; number of neurospheres formed by Met^{high} or Met^{neg} cells after 14 days with (+) or without (−) HGF. §, 2-sided *t*test, $P < 0.05$. C, flow cytometry; expression of *Sox2* or Nestin in BT308 neurosphere in standard medium (SM) with or without HGF. §, 2-sided *t* test,$P < 0.05$. D, qPCR; expression of *Nanog* and *Sox2* in neurospheres treated with HGF with respect to standard medium (Ctrl).

Moreover, HGF supported the clonogenic ability of Met^{high} cells, sorted as single cells from Met-pos-NS and cultured in the presence or in the absence of HGF as the sole growth factor (Fig. 4B). Conversely, HGF did not stimulate neurosphere formation by Met^{neg} cells (Fig. 4B). Accordingly, in Met-pos-NS, addition of HGF significantly increased the number of $Sox2^{pos}$ or $Nestin^{pos}$ cells (Fig. 4C and Supplementary Fig. S9B) and transcription of self-renewal markers *Sox2, Nanog, CD133*, and *EZH2* (Fig. 4Dand Supplementary Fig. S9C), as compared with standard medium. Taken together, these data indicated that HGF sustains the stem-like phenotype of Met-pos-NS.Met signaling has been associated with induction of epithelial–mesenchymal transition and the "invasive growth" program (32–34). We thus investigated whether HGF supported the invasive properties of neurospheres. In transwell assays, addition of HGF to standard medium strikingly enhanced migration and invasion of Met-pos-NS (Fig. 5A and B and data not shown). This effect was completely abolished by specific Met inhibitors, including the Fab fragment of the anti-Met antibody DN30 (ref. 35; Fig. 5C) or the specific tyrosine kinase inhibitor JNJ-38877605 (ref. 14; Supplementary Fig. S9D). As expected, HGF did not increase migration or invasion of Met-neg-NS

(Fig. 5A and B). In these cells, transfection of Met did not promote invasiveness *per se* but conferred the ability to respond to HGF (Fig. 5D).

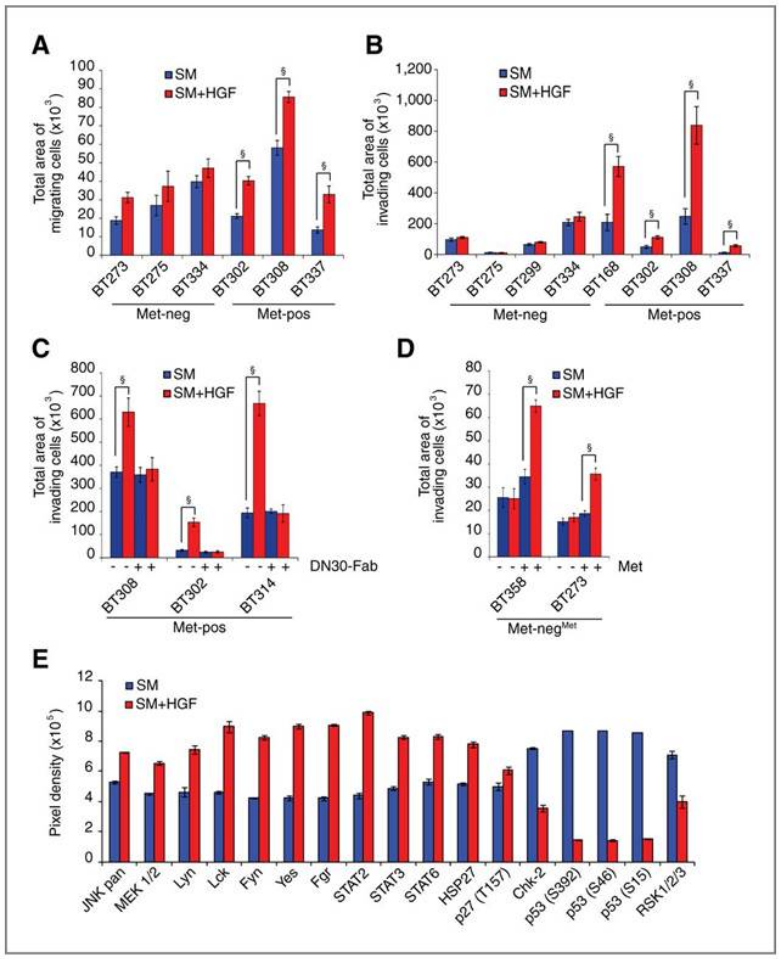

Figure 5.
HGF sustains invasive growth. A and B, transwell assay; neurospheres were dissociated and analyzed for migration (without Matrigel coating, A) or invasion (with Matrigel coating, B) in standard medium with or without HGF. §, 2-sided *t* test, $P < 0.05$. C, neurospheres assessed as in B, with (+) or without (−) anti-Met antibodies (DN30-Fab). §, 2-sided *t* test, $P < 0.05$. D, representative Met-neg-NS transfected (+) or not (−) with Met and assessed as in B. §, 2-sided *t* test, $P< 0.05$. E, phosphorylation of intracellular signal transduces in BT308 neurosphere cultured in standard medium with or without HGF for 24 hours. Statistically significantly modulated proteins were represented (2-sided *t* test,$P < 0.05$).

Analysis of intracellular phosphoprotein arrays, showed that, in Met-pos-NS, HGF induced phosphorylation of signal transducers known to control cell invasion, such as JNK, MEK 1/2, several members of Src and STAT families, and p27 (ref. 34; Fig. 5E). Interestingly, the latter was phosphorylated at a residue (T157) that promotes cytoplasmic localization and activation of the cell migratory machinery (36). We also observed decreased phosphorylation of p53 at residues Ser15, Ser46, and Ser392, which results in p53 inhibition (37).

Taken together, these results showed that Met activation by HGF concomitantly supports the stem-like and the invasive phenotype of Met-pos-NS *in vitro* and suggest that this mechanism may promote aggressiveness of a subset of glioblastomas.

Discussion

A unifying model of tumor onset and progression that integrates the CSC model and the Darwinian model assumes that CSCs accumulate the driving genetic lesions and transmit them to the genetically and phenotypically heterogeneous progeny forming the tumor bulk (38). The comparative analysis reported in this article showed that, as a rule, the same mutations of primary glioblastomas are found in their matched neurospheres. This confirms that neurospheres are a faithful *in vitro* model of the original tumor, useful to dissect the relationship between genetics and biology, and to predict the therapeutical response.

Notably, neurospheres derived from $EGFR^{amp/vIII}$ tumors displayed a decreased—or in a few cases an even normal—number of *EGFR* gene copies, consistent with previous and recent data (17, 18). As *EGFR* amplification is usually detected only in a fraction of glioblastoma cells (data not shown and ref. 39), these findings can be explained by *in vitro* negative selection of clones harboring *EGFR* amplification and positive selection of clones with a normal *EGFR* gene, coexisting in the same tumor. Growth of clones with normal/low number of *EGFR* gene copies might be favored by concentrations of exogenous EGF (20 ng/mL), likely exceeding those in brain tissues (18).

Gene expression profiling allowed to classify the neurospheres into classical, mesenchymal, and proneural subtypes according to the signatures identified in glioblastoma tissues by Verhaak (6). Interestingly, the classical subgroup encompassed the vast majority of neurospheres harboring *EGFR* amplification (7 of 10), confirming an association between the classical expression profile and *EGFR* genetic alteration already observed in tumors (6). *Vice versa*, the mesenchymal/proneural subgroup included neurospheres mostly harboring a wild-type *EGFR* gene (7 of 8), together with deletion/mutation of *PTEN* tumor suppressor gene (6 of 8). This association—to our knowledge—was still unreported in tumors or neurospheres.

EGFR is renowned as a prominent player of glioma biology (40) and tumorigenic potential of glioblastoma stem cells (41). However, we found that EGFR was highly expressed in classical neurospheres, consistent with the presence of gene amplification, but barely detectable in most mesenchymal/proneural neurospheres. In search for a functional marker for glioblastoma stem cells lacking EGFR, we considered the *MET* oncogene. Indeed, we noticed that *MET* was listed among genes upregulated in microarrays of glioblastoma tissues, in association with the mesenchymal subtype (6). Moreover, recently, Met was shown to support the stem-like phenotype of unclassified glioblastoma neurospheres (42). The data presented in this article show, for the first time, that Met expression is preferentially associated with the mesenchymal/proneural subtype of glioblastoma stem cells, and that expression of EGFR and Met are mutually exclusive in neurospheres and, possibly, in original tumors. If further studies will confirm that the cellular distribution of Met and EGFR in patients reflects that observed in neurospheres, there will be far-reaching implications for the molecular diagnostics of glioblastoma. Flow cytometric or immunohistochemical analysis of the EGFR-Met pair could be proposed as a reliable test to discriminate between classical and mesenchymal/proneural glioblastoma, possibly in addition to previous criteria, such as YKL-40 expression (5).

Interestingly, the neurosphere subgroup expressing Met (Met-pos-NS), irrespective of their mesenchymal or proneural profile, and the subgroup lacking Met (Met-neg-NS) displayed significant biologic differences. They had a different proliferation rate, invariably higher in Met-pos-NS. In this respect, the 2 subgroups were reminiscent of those previously described (12). Interestingly, Met-pos-NS mostly proliferated even without growth factors, and, as expected, were insensitive to EGF, whereas Met-neg-NS depended on exogenous growth factor, mostly EGF. Moreover, the 2 neurosphere subgroups showed a divergent differentiation pattern, either *in vitro*, or in tumors formed by orthotopic transplantation: Met-pos-NS differentiated along the neuro-astroglial, whereas Met-neg-NS along the neuro-oligodendroglial pathway. These findings seem

consistent with observations in mouse model systems, in which brain progenitors inheriting high levels of EGFR give rise to astrocytes, whereas those inheriting low levels generate oligodendrocytes (43).

Strikingly, the Met-pos and Met-neg neurosphere subgroups not only displayed distinct biologic features but were conserved according to 5 additional transcriptional classifiers, obtained in neurospheres or in original tumors (5, 26–29). When 2-cluster classifiers found in neurospheres by Gunther and colleagues (26) or Lottaz and colleagues (27) were applied, Met-neg-NS almost fully overlapped with Cluster I/Type I, whereas Met-pos-NS overlapped with Cluster II/Type II.

Taken together, biologic and gene expression features of Met-pos and Met-neg neurospheres suggest that Met expression could associate with tumors deriving from different cells of origin. Met-neg-NS (and glioblastoma) could derive from stem or transit amplifying cells of the brain subventricular zone, which depend on EGFR signaling (8, 44). Conversely, Met-pos-NS (and glioblastoma) could originate either from the subventricular progenitors inheriting low levels of EGFR (43), or the diffuse astrocytes of the reactive glia. These cells reactivate their proliferative and regenerative potential in response to injuries (45). The reactive astrocytes are an appealing candidate as a glioblastoma cell-of-origin, also because they are intermingled within the blood–brain barrier and may be easily exposed to genotoxic agents.

Another novel finding presented in this study is that, in each Met-pos-NS, Met marks and functionally supports a cell subpopulation that retains long-term clonogenic and multipotential ability *in vitro* and enhanced growth kinetics *in vivo* and thus may retain cancer stem cell properties. Conversely, in Met-pos-NS, loss of Met expression characterizes a cell subpopulation that exhausts its clonogenic activity *in vitro* and *in vivo*. These data strongly suggest that Met is a glioblastoma stem cell marker, which can be proposed for cell isolation as an alternative to CD133.

A further new finding presented in this study indicates that Met supports not only the stem-like but also the invasive phenotype, at least *in vitro*. Indeed, invasiveness of Met-pos-NS was significantly enhanced by the Met ligand HGF, a key driver of invasive growth (32), and counteracted by specific Met inhibitors. The Met ability to concomitantly support stemness and invasiveness shows that the two phenotypes are functionally associated and driven by the same signaling circuits and genetic programs, consistent with previous observations (46).

It has been noticed that “the existence of molecularly defined subgroups of glioblastoma raises the question of whether these categories actually represent separate disease entities rather than the expression of minor variability in a single tumor class (15).” Our study suggests that primary glioblastomas contain distinct types of CSCs, each possibly arising from distinct cells of origin, each endowed with specific molecular markers and signaling circuits responsible for stem and tumorigenic properties. These findings contribute to identify separate glioblastoma entities and to define criteria that might be exploited to guide therapeutic decision making.

Disclosure of Potential Conflicts of Interest

No potential conflicts of interest were disclosed.

Grant Support

The study was supported by Italian Association for Cancer Research (Investigator Grants and “Special Program Molecular Clinical Oncology 5xMille, N. 9970”), Regione Piemonte (PI-STEM), European Union Framework Programs 7 (N. 201279 and 201640).

The costs of publication of this article were defrayed in part by the payment of page charges. This article must therefore be hereby marked *advertisement* in accordance with 18 U.S.C. Section 1734 solely to indicate this fact.

Acknowledgments

The authors thank Andrea Bertotti, Livio Trusolino, and Claudio Isella for critical discussion; Stefania Giove for histopathology; Daniela Gramaglia, Antonella Cignetto, and Michela Bruno for secretarial assistance.

References

1.Wen PY, Kesari S. Malignant gliomas in adults. N Engl J Med 2008;359:492–507.

2. Comprehensive genomic characterization defines human glioblastoma genes and core pathways. Nature 2008;455:1061–8.

3. Brennan C, Momota H, Hambardzumyan D, Ozawa T, Tandon A, Pedraza A, et al. Glioblastoma subclasses can be defined by activity among signal transduction pathways and associated genomic alterations. PLoS One 2009;4:e7752.

4. Parsons DW, Jones S, Zhang X, Lin JC, Leary RJ, Angenendt P, et al. An integrated genomic analysis of human glioblastoma multiforme. Science2008;321:1807–12.

5. Phillips HS, Kharbanda S, Chen R, Forrest WF, Soriano RH, Wu TD, et al. Molecular subclasses of high-grade glioma predict prognosis, delineate a pattern of disease progression, and resemble stages in neurogenesis. Cancer Cell 2006;9:157–73.

6. Verhaak RG, Hoadley KA, Purdom E, Wang V, Qi Y, Wilkerson MD, et al. Integrated genomic analysis identifies clinically relevant subtypes of glioblastoma characterized by abnormalities in PDGFRA, IDH1, EGFR, and NF1. Cancer Cell2010;17:98–110.

7. Yan H, Parsons DW, Jin G, McLendon R, Rasheed BA, Yuan W, et al. IDH1 and IDH2 mutations in gliomas. N Engl J Med 2009;360:765–73.

8. Vescovi AL, Galli R, Reynolds BA. Brain tumour stem cells. Nat Rev Cancer2006;6:425–36.

9. Dirks PB. Brain tumor stem cells: bringing order to the chaos of brain cancer. J Clin Oncol 2008;26:2916–24.

10. Bao S, Wu Q, McLendon RE, Hao Y, Shi Q, Hjelmeland AB, et al. Glioma stem cells promote radioresistance by preferential activation of the DNA damage response.Nature 2006;444:756–60.

11. Park CY, Tseng D, Weissman IL. Cancer stem cell-directed therapies: recent data from the laboratory and clinic. Mol Ther 2009;17:219–30.

12. Galli R, Binda E, Orfanelli U, Cipelletti B, Gritti A, De VS, et al. Isolation and characterization of tumorigenic, stem-like neural precursors from human glioblastoma.Cancer Res 2004;64:7011–21.

13. Louis DN, Ohgaki H, Wiestler OD, Cavenee WK, Burger PC, Jouvet A, et al. The 2007 WHO classification of tumours of the central nervous system. Acta Neuropathol2007;114:97–109.

14. De Bacco F, Luraghi P, Medico E, Reato G, Girolami F, Perera T, et al. Induction of MET by ionizing radiation and its role in radioresistance and invasive growth of cancer.J Natl Cancer Inst 2011;103:645–61.

15. Huse JT, Holland EC. Targeting brain cancer: advances in the molecular pathology of malignant glioma and medulloblastoma. Nat Rev Cancer 2010;10:319–31.

16. Bredel M, Scholtens DM, Yadav AK, Alvarez AA, Renfrow JJ, Chandler JP, et al. NFKBIA deletion in glioblastomas. N Engl J Med 2011;364:627–37.

17. Pandita A, Aldape KD, Zadeh G, Guha A, James CD. Contrasting *in vivo* and *in vitro* fates of glioblastoma cell subpopulations with amplified EGFR. Genes Chromosomes Cancer 2004;39:29–36.

18. Schulte A, Gunther HS, Martens T, Zapf S, Riethdorf S, Wulfing C, et al. Glioblastoma stem-like cell lines with either maintenance or loss of high-level EGFR amplification, generated via modulation of ligand concentration. Clin Cancer Res2012;18:1901–13

19.Koochekpour S, Jeffers M, Rulong S, Taylor G, Klineberg E, Hudson EA, et al. Met and hepatocyte growth factor/scatter factor expression in human gliomas. Cancer Res 1997;57:5391–8.

20. Kong DS, Song SY, Kim DH, Joo KM, Yoo JS, Koh JS, et al. Prognostic significance of c-Met expression in glioblastomas. Cancer 2009;115:140–8.

21. Singh SK, Hawkins C, Clarke ID, Squire JA, Bayani J, Hide T, et al. Identification of human brain tumour initiating cells. Nature 2004;432:396–401.

22. Beier D, Hau P, Proescholdt M, Lohmeier A, Wischhusen J, Oefner PJ, et al. CD133(+) and CD133(−) glioblastoma-derived cancer stem cells show differential growth characteristics and molecular profiles. Cancer Res 2007;67:4010–5.

23. Chen R, Nishimura MC, Bumbaca SM, Kharbanda S, Forrest WF, Kasman IM, et al. A hierarchy of self-renewing tumor-initiating cell types in glioblastoma. Cancer Cell2010;17:362–75.

24. Doetsch F. The glial identity of neural stem cells. Nat Neurosci 2003;6:1127–34.

25. Pruszak J, Ludwig W, Blak A, Alavian K, Isacson O. CD15, CD24, and CD29 define a surface biomarker code for neural lineage differentiation of stem cells. Stem Cells 2009;27:2928–40.

26. Gunther HS, Schmidt NO, Phillips HS, Kemming D, Kharbanda S, Soriano R, et al. Glioblastoma-derived stem cell-enriched cultures form distinct subgroups according to molecular and phenotypic criteria. Oncogene 2008;27:2897–909.

27. Lottaz C, Beier D, Meyer K, Kumar P, Hermann A, Schwarz J, et al. Transcriptional profiles of CD133+ and CD133- glioblastoma-derived cancer stem cell lines suggest different cells of Origin. Cancer Res 2010;70:2030–40.

28. Freije WA, Castro-Vargas FE, Fang Z, Horvath S, Cloughesy T, Liau LM, et al. Gene expression profiling of gliomas strongly predicts survival. Cancer Res2004;64:6503–10.

29. Schulte A, Gunther HS, Phillips HS, Kemming D, Martens T, Kharbanda S, et al. A distinct subset of glioma cell lines with stem cell-like properties reflects the transcriptional phenotype of glioblastomas and overexpresses CXCR4 as therapeutic target. Glia 2011;59:590–602.

30. Li Y, Guessous F, Zhang Y, Dipierro C, Kefas B, Johnson E, et al. MicroRNA-34a inhibits glioblastoma growth by targeting multiple oncogenes. Cancer Res2009;69:7569–76.

31. Salvi A, Sabelli C, Moncini S, Venturin M, Arici B, Riva P, et al. MicroRNA-23b mediates urokinase and c-met downmodulation and a decreased migration of human hepatocellular carcinoma cells. FEBS J 2009;276:2966–82.

32. Boccaccio C, Comoglio PM. Invasive growth: a MET-driven genetic programme for cancer and stem cells. Nat Rev Cancer 2006;6:637–45.

33. Thiery JP, Acloque H, Huang RY, Nieto MA. Epithelial-mesenchymal transitions in development and disease. Cell 2009;139:871–90.

34. Trusolino L, Bertotti A, Comoglio PM. MET signalling: principles and functions in development, organ regeneration and cancer. Nat Rev Mol Cell Biol 2010;11:834–48.

35. Petrelli A, Circosta P, Granziero L, Mazzone M, Pisacane A, Fenoglio S, et al. Ab-induced ectodomain shedding mediates hepatocyte growth factor receptor down-regulation and hampers biological activity. Proc Natl Acad Sci U S A 2006;103:5090–5.

36. Larrea MD, Wander SA, Slingerland JM. p27 as Jekyll and Hyde: regulation of cell cycle and cell motility. Cell Cycle 2009;8:3455–61.

37. Dai C, Gu W. p53 post-translational modification: deregulated in tumorigenesis.Trends Mol Med 2010;16:528–36.

38. Dick JE. Stem cell concepts renew cancer research. Blood 2008;112:4793–807.

39. Strommer K, Hamou MF, Diggelmann H, de TN. Cellular and tumoural heterogeneity of EGFR gene amplification in human malignant gliomas. Acta Neurochir (Wien) 1990;107:82–7.

40. Nicholas MK, Lukas RV, Jafri NF, Faoro L, Salgia R. Epidermal growth factor receptor–mediated signal transduction in the development and therapy of gliomas. Clin Cancer Res 2006;12:7261–70.

41. Mazzoleni S, Politi LS, Pala M, Cominelli M, Franzin A, Sergi SL, et al. Epidermal growth factor receptor expression identifies functionally and molecularly distinct tumor-initiating cells in human glioblastoma multiforme and is required for gliomagenesis.Cancer Res 2010;70:7500–13.

42. Li Y, Li A, Glas M, Lal B, Ying M, Sang Y, et al. c-Met signaling induces a reprogramming network and supports the glioblastoma stem-like phenotype. Proc Natl Acad Sci U S A 2011;108:9951–6.

43. Sun Y, Goderie SK, Temple S. Asymmetric distribution of EGFR receptor during mitosis generates diverse CNS progenitor cells. Neuron 2005;45:873–86.

44. Pastrana E, Cheng LC, Doetsch F. Simultaneous prospective purification of adult subventricular zone neural stem cells and their progeny. Proc Natl Acad Sci U S A2009;106:6387–92.

45. Robel S, Berninger B, Gotz M. The stem cell potential of glia: lessons from reactive gliosis. Nat Rev Neurosci 2011;12:88–104.

46. Mani SA, Guo W, Liao MJ, Eaton EN, Ayyanan A, Zhou AY, et al. The epithelial-mesenchymal transition generates cells with properties of stem cells. Cell2008;133:704–15.